Hindawi
Mathematical Problems in Engineering
Volume 2023, Article ID 3916279, 8 pages
https://doi.org/10.1155/2023/3916279

Research Article

Stabilization of Double Inverted Pendulum Systems Based on Hierarchical Sliding Mode Control Techniques

Muhammad Idrees,[1] Zia Ullah ,[2] Jihad Younis ,[3] Sohail Ahmad,[2] and Hafeez Ahmad[4]

[1]*Department of Mathematics and Statistics, The University of Lahore, Lahore, Pakistan*
[2]*Department of Mathematics and Statistics, The University of Lahore, Sargodha Campus, Sargodha 40100, Pakistan*
[3]*Aden University, Khormaksar, P. O. Box. 6014, Aden, Yemen*
[4]*Department of Statistics, School of Quantitative Sciences, University Utara, Sintok, Malaysia*

Correspondence should be addressed to Jihad Younis; jihadalsaqqaf@gmail.com

Received 23 February 2023; Revised 20 June 2023; Accepted 25 July 2023; Published 18 August 2023

Academic Editor: Sundarapandian Vaidyanathan

The double rotary inverted pendulum (DRIP) system belongs to the class of under-actuated mechanical systems, and it is a highly nonlinear, unstable, and benchmark system to test the different control techniques. This paper successfully designed the nonlinear hierarchical sliding mode control (HSMC) techniques to stabilize the DRIP system. We compare the performance of these techniques numerically with each other and with the previously designed control technique. We propose an aggregated HSMC technique as it has a much shorter stabilization time than other designed techniques.

1. Introduction

Sliding mode control (SMC) is a nonlinear control technique that changes nonlinear system dynamics by implementing an appropriate control signal. This control signal force the system to slide along a sliding surface. It was first applied in the 1960s, and its primary formulation is based on the work of Utkin and Korovin [1]. Utkin introduced the concept of the sliding surface from which equivalent control is obtained. After this, Utkin and Yang [2] proceeded with their work and designed a nonlinear switching term that guarantees the robustness of SMC. The use of the Lyapunov function ensures the robustness of SMC that intensify it on other control techniques. SMC technique can deal with complex higher-order systems and has been applied to control the different mechanical systems.

Inverted pendulum systems are members of under-actuated mechanical systems and are well known for implementing and validating newly designed control techniques [3–5]. The rotary inverted pendulum (RIP) system is a type inverted pendulum system that is strongly nonlinear and well suited to compare the performance of different control techniques. It has many applications in the field of robotics, controlling satellite and aerospace vehicles, etc. Researchers have proposed many control methodologies to solve the stabilization problem for RIPs. Furuta et al. [6] used pseudostate feedback method for swing-up control of inverted pendulum. Choi and Kim [7] introduced the long-lasting control for rotational inverted pendulum employing a feedback sliding mode controller. They presented system modeling, design controller, and execution of controller to inverted rotational pendulum system. Pakdeepattarakorn et al. [8] introduced dynamic models of a double rotary inverted pendulum (DRIP) system. Driver and Thorpe [9] designed control of rotary single/double inverted pendulum. Casanova et al. [10] worked on the development and control structure of DRIP by using multiple feedback delay. Li [11] worked on a rotational double inverted pendulum system by developing a mathematical model using the Euler Lagrange align and used the DAFC (direct adaptive fuzzy control) method to increase LQR (linear quadratic regulator) performance to stabilize the system. Jose et al. [12] worked to balance the pendulum in its upwards position by using proportional integral derivative and LQR control techniques on comparison based. Yue et al. [13] worked on nonholonomic/under-actuated wheeled inverted pendulum vehicle based on a data-driven trajectory devisor by applying an indirect adaptive fuzzy control technique.

Wen et al. [14] controlled RIP system based on logarithmic Lyapunov function. A logarithmic function is built as the function of Lyapunov and contrasted with the normal quadratic function [14]. They used the linearized model that may influence controller performance because the RIP system is highly nonlinear. Liu et al. [15] proposed stabilization two dimensional stochastic systems through SMC. Idrees et al. [16] discussed hierarchical sliding mode control (HSMC) and decoupled sliding mode controller to mark the stabilization problem and demonstrated powerful HSMC with state-dependent switching gain for stabilization of RIP. Markazi et al. [17] presented adaptive fuzzy SMC of under-actuated nonlinear system. Using logical switching and integral SMC, Butt [18] suggested rigorous stability of a class of nonholonomic/under-actuated structures. To balance the system, a switching containing three distinct steps was used [18]. Mehedi et al. [19] used fractional order integral control scheme for the stabilization of DRIP system. All the discussed control techniques are either designed for a single pendulum RIP system or complicated with a large stabilization time to stabilize DRIP system. This paper aims to provide an efficient control technique having the less computational burden to stabilize the DRIP system. For this purpose, we design three different HSMC techniques to stabilize DRIP system and compare their performances.

2. Mathematical Model of Double Inverted Rotary Pendulum

DRIP is a highly nonlinear, unstable, and challenging control system. It can be divided into three subsystems as shown in Figure 1.

Two pendulums are stacked on top of one another and mounted on a horizontal bar, controlled and stabilized through an appropriate control input. The dynamics of DRIP system can be presented mathematically as follows:

$$\begin{aligned}&(J_1 + L_1^2(m_2+m_3))\,\ddot{\Theta}_1 + L_1(m_2 l_2 + m_3 L_2)\cos\Theta_2\,\ddot{\Theta}_2\\&+L_1 m_3 l_3\cos\Theta_3\,\ddot{\Theta}_3 + b_1\dot{\Theta}_1 - L_1(m_2 l_2 + m_3 L_2)\dot{\Theta}_1^2\sin\Theta_2\\&-L_1 m_3 l_3\dot{\Theta}_3^2\sin\Theta_2 = \tau,\end{aligned} \tag{1}$$

$$\begin{aligned}&-L_1(m_2 l_2 + m_3 L_2)\cos\Theta_2\,\ddot{\Theta}_1 - (J_2 + L_2^2 m_3 + m_2 l_2^2)\,\ddot{\Theta}_2\\&-L_2 m_3 l_3\cos(\Theta_3-\Theta_2)\,\ddot{\Theta}_3 - b_2\dot{\Theta}_2 + L_2 m_3 l_3\dot{\Theta}_3^2\sin(\Theta_3-\Theta_2)\\&+(m_2 l_2 + m_3 L_2)g\sin\Theta_2 = 0,\end{aligned} \tag{2}$$

$$\begin{aligned}&-L_1 m_3 l_3\cos\Theta_3\,\ddot{\Theta}_1 - L_2 m_3 l_3\cos(\Theta_3-\Theta_2)\,\ddot{\Theta}_2 - (J_3 + l_3^2 m_3)\,\ddot{\Theta}_3\\&-b_3\dot{\Theta}_3 - L_2 m_3 l_3\dot{\Theta}_2^2\sin(\Theta_3-\Theta_2) + m_3 l_3 g\sin\Theta_3 = 0,\end{aligned} \tag{3}$$

where Θ_1, Θ_2, and Θ_3 are angles of horizontal, first, and second vertical bars, respectively. The above dynamic Equations. (1)–(3) can be rewritten as follows:

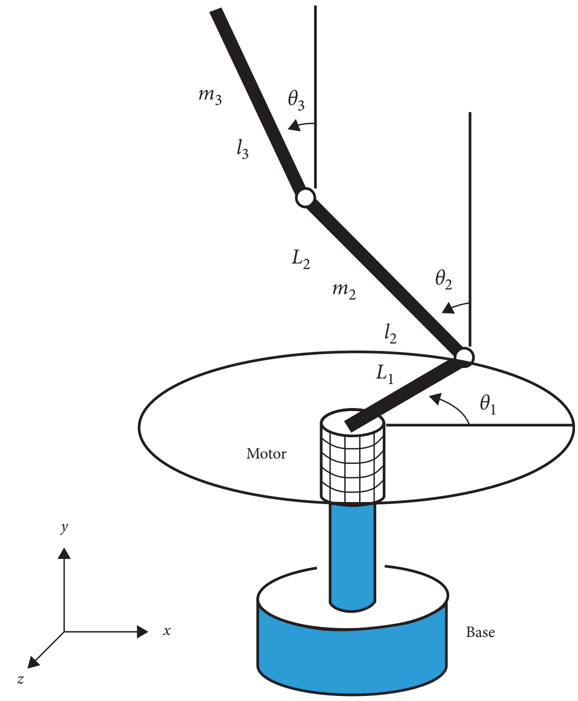

Figure 1: Schematic design of double inverted rotary pendulum.

$$\begin{aligned}H_1\,\ddot{\Theta}_1 &= \tau - b_1\dot{\Theta}_1 - H_2\,\ddot{\Theta}_2\cos\Theta_2 - H_3\,\ddot{\Theta}_3\cos\Theta_3\\&\quad + H_2\dot{\Theta}_2^2\sin\Theta_2 + H_3\dot{\Theta}_3^2\sin\Theta_3,\end{aligned} \tag{4}$$

$$\begin{aligned}H_4\,\ddot{\Theta}_2 &= -b_2\dot{\Theta}_2 - H_2\,\ddot{\Theta}_1\cos\Theta_2 - H_5\,\ddot{\Theta}_3\cos(\Theta_3-\Theta_2)\\&\quad + H_5\dot{\Theta}_3^2\sin(\Theta_3-\Theta_2) + H_7\sin\Theta_2,\end{aligned} \tag{5}$$

$$\begin{aligned}H_6\,\ddot{\Theta}_3 &= -b_3\dot{\Theta}_3 - H_3\,\ddot{\Theta}_1\cos\Theta_3 - H_5\,\ddot{\Theta}_2\cos(\Theta_3-\Theta_2)\\&\quad - H_5\dot{\Theta}_2^2\sin(\Theta_3-\Theta_2) + H_8\sin\Theta_3.\end{aligned} \tag{6}$$

Here J_1 is the momentum of inertia around the rotation of the horizontal bar, J_2 is the momentum of inertia of the first pendulum, J_3 is the momentum of inertia of the second pendulum, L_1 is the length of the horizontal bar, L_2 is the length of the first pendulum, m_2 is the mass of first pendulum, m_3 is the mass of second pendulum, g is the gravitational acceleration, and τ is control input. H_1, H_2, H_3, H_4, H_5, H_6, H_7, and H_8 are defined in the appendix. The state-space representation of DRIP system is given by

$$\begin{aligned}\dot{y}_1 &= y_2,\\ \dot{y}_2 &= F_1(y) + G_1(y)\tau,\\ \dot{y}_3 &= y_4,\\ \dot{y}_4 &= F_2(y) + G_2(y)\tau,\\ \dot{y}_5 &= y_6,\\ \dot{y}_6 &= F_3(y) + G_3(y)\tau,\end{aligned} \tag{7}$$

where y_1 is the angle of horizontal bar making with x-axis, y_2 is the angular velocity of the horizontal bar, y_3 is the angle of the first pendulum making with y-axis, y_4 is the angular velocity of the first pendulum, y_5 is the angle of the second pendulum making with y-axis, and y_6 is the angular velocity of the second pendulum. $F_1(y)$, $F_2(y)$, $F_3(y)$, $G_1(y)$, $G_2(y)$, and $G_3(y)$ are nonlinear functions defined by $F_i(y) = \alpha_i(y)/\Delta$ and $G_i(y) = \beta_i(y)/\Delta$ $(i = 1, 2, 3)$. Here α, β, and Δ are also nonlinear functions defined in the appendix.

3. Hierarchical Sliding Mode Control

In most circumstances, there is inaccuracy between the actual plant and its mathematical model. This inconsistency is due to the external disturbances, parameters variations, and unmodeled dynamics of the plant. Due to these reasons designing a control law is a challenging problem. SMC is a particular type of variable structure control system that forces the system's state to reach a certain manifold and subsequently to remain on a specified surface within the state space. This manifold is called a sliding surface. The sliding surface is a function of the state variables. Once the sliding surface is reached, SMC keeps the system states on the closed neighborhood of the sliding surface. SMC uses a finite amount of time to force the system trajectories to move along the sliding surface. In this section, we will design three different HSMC techniques to stabilize the DRIP system.

3.1. Control Law Based on Aggregated HSMC. The DRIP system consists of three subsystems, and each subsystem contains two state variables. The basic idea behind the design of aggregated HSMC is to construct three first-level sliding surfaces, and each first-level sliding surface is a linear combination of two state variables. These first-level sliding surfaces are aggregated to construct a second-level sliding surface. The schematic diagram of aggregated HSMC is shown in Figure 2.

To design controller for DRIP system based on aggregated HSMC, we consider state-space representation Equation (7) and define first-level sliding surfaces as

$$\begin{aligned} s_1 &= c_1 y_1 + c_2 y_2, \\ s_2 &= c_3 y_3 + c_4 y_4, \\ s_3 &= c_5 y_5 + c_6 y_6, \end{aligned} \tag{8}$$

where c_i $(i = 1, 2, .., 6)$ are positive constants. To design the higher order sliding surface, we aggregate these three layers of sliding surfaces as follows:

$$S = \alpha_1 s_1 + \alpha_2 s_2 + \alpha_3 s_3, \tag{9}$$

where α_i $(i = 1, 2, 3)$ are constants. Aggregated control law is defined by

$$\tau = \tau_{eq1} + \tau_{eq2} + \tau_{eq3} + \tau_{sw}. \tag{10}$$

To obtain equivalent control law of three subsystems, we take $\dot{s_i} = 0$ then

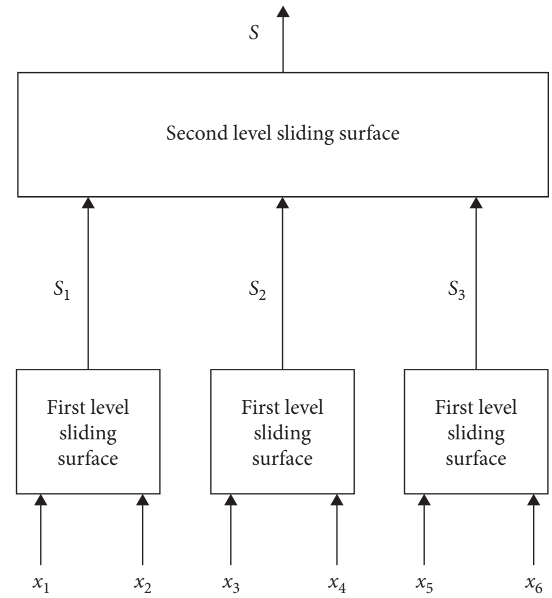

Figure 2: Structure of the aggregated sliding surfaces.

$$\tau_{eq1} = \frac{-c_1 y_2 - c_2 F_1(y)}{c_2 G_1(y)}, \tag{11}$$

$$\tau_{eq2} = \frac{-c_3 y_4 - c_4 F_2(y)}{c_4 G_2(y)}, \tag{12}$$

$$\tau_{eq3} = \frac{-c_5 y_6 - c_6 F_3(y)}{c_6 G_3(y)}. \tag{13}$$

Now we design the switching control law by using Lyapunov function as follows:

$$V = \frac{1}{2} S^2. \tag{14}$$

Differentiating Lyapunov function w.r.t t,

$$\begin{aligned} \dot{V} &= S\dot{S}, \\ \dot{V} &= S[\alpha_1 \dot{s}_1 + \alpha_2 \dot{s}_2 + \alpha \dot{s}_3], \\ \dot{V} &= S\big[\alpha_1 (c_1 y_2 + c_2 F_1(y) + c_2 G_1(y)\big(\tau_{eq1} + \tau_{eq2} + \tau_{eq3} + \tau_{sw}\big) \\ &\quad + \alpha_2 (c_3 y_4 + c_4 F_2(y) + c_4 G_2(y)\big(\tau_{eq1} + \tau_{eq2} + \tau_{eq3} + \tau_{sw}\big) \\ &\quad + \alpha_3 (c_5 y_6 + c_6 F_3(y) + c_6 G_3(y)\big(\tau_{eq1} + \tau_{eq2} + \tau_{eq3} + _{sw}\big)\big]. \end{aligned} \tag{15}$$

By substituting Equations. (11)–(13) into above expression, we have

$$\dot{V} = S[\alpha_1 c_2 G_1(y) + \alpha_2 c_4 G_2(y) + \alpha_3 c_6 G_3(y)]. \tag{16}$$

We define $\dot{S}$ as follows:

$$\dot{S} = -\epsilon \cdot \text{sat}(S), \tag{17}$$

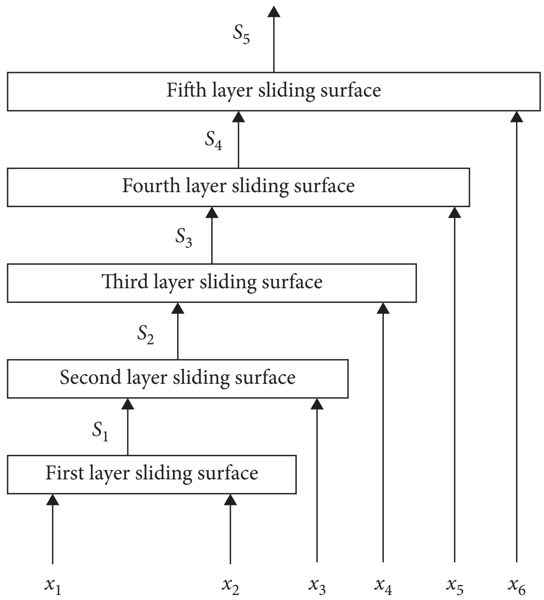

FIGURE 3: Structure of the incremental sliding surfaces.

$$\dot{V} = S[-\epsilon \cdot \mathrm{sat}(S)]. \tag{18}$$

The switching control is obtained from align Equations (16) and (18) as follows:

$$\tau_{sw} = \frac{-\epsilon \cdot \mathrm{sat}(S)}{\alpha_1 c_2 G_1(y) + \alpha_2 c_4 G_2(y) + \alpha_3 c_6 G_3(y)}. \tag{19}$$

3.2. Control Law Based on Incremental HSMC. In incremental HSMC, we select arbitrary two state variables to design the first layer of the sliding surface. The second layer of the sliding surface is constructed by increasing one variable in the first layer. This proceeds till all the system state variables are included. As the crane model covers six state variables, the incremental sliding surfaces will consist of five layers. The schematic presentation of incremental HSMC is shown in Figure 3.

The first layer of sliding surface is defined as follows:

$$s_1 = \zeta_1 y_1 + \zeta_2 y_2, \tag{20}$$

$$\dot{s}_1 = \zeta_1 \dot{y}_1 + \zeta_2 \dot{y}_2, \tag{21}$$

$$\dot{s}_1 = \zeta_1 y_2 + \zeta_2 [F_1(y) + G_1(y)\tau], \tag{22}$$

where ζ_1 and ζ_2 are positive constant. Now second layer of sliding surface s_2 is constructed by the linear combination of the first sliding surface s_1 and third state variable y_3 as follows:

$$\begin{aligned} s_2 &= \zeta_3 y_3 + s_1. \\ \dot{s}_2 &= \zeta_3 \dot{y}_3 + \dot{s}_1, \\ \dot{s}_2 &= \zeta_3 y_4 + \zeta_1 y_2 + \zeta_2 [F_1(y) + G_1(y)\tau]. \end{aligned} \tag{23}$$

Third layer of sliding surface can be defined by

$$\begin{aligned} s_3 &= \zeta_4 y_4 + s_2, \\ \dot{s}_3 &= \zeta_4 \dot{y}_4 + \dot{s}_2. \end{aligned} \tag{24}$$

Fourth layer of sliding surface can be defined by

$$\begin{aligned} s_4 &= \zeta_5 y_5 + s_3, \\ \dot{s}_4 &= \zeta_5 \dot{y}_5 + \dot{s}_3. \end{aligned} \tag{25}$$

Fifth layer of sliding surface can be defined by

$$\begin{aligned} s_5 &= \zeta_6 y_6 + s_4, \\ \dot{s}_5 &= \zeta_6 \dot{y}_6 + \dot{s}_4, \\ \dot{s}_5 &= \zeta_6 [F_3(y) + G_3(y)\tau] + \zeta_5 y_6 + \zeta_4 [F_2(y) + G_2(y)\tau] \\ &\quad + \zeta_3 y_4 + \zeta_1 y_2 + \zeta_2 [F_1(y) + G_1(y)\tau]. \end{aligned} \tag{26}$$

The incremental control law is defined by

$$\tau = \tau_{eq} + \tau_{sw}. \tag{27}$$

The equivalent control is obtained by putting $\dot{s}_5 = 0$ as follows:

$$\tau_{eq} = \frac{-\zeta_5 y_6 - \zeta_3 y_4 - \zeta_1 y_2 - \zeta_2 F_1(y) - \zeta_4 F_2(y) - \zeta_6 F_3(y)}{\zeta_2 G_1(y) + \zeta_4 G_2(y) + \zeta_6 G_3(y)}. \tag{28}$$

The switching control law can be obtained by defining Lyapunov function as follows:

$$V = \frac{1}{2} s_5^2, \tag{29}$$

$$\dot{V} = s_5 \dot{s}_5. \tag{30}$$

Using expression of Equations (26) and (27),

$$\begin{aligned} \dot{V} &= s_5 [\zeta_6 F_3(y) + \zeta_4 F_2(y) + \zeta_2 F_1(y) + \zeta_5 y_6 + \zeta_3 y_4 + \zeta_1 y_2 \\ &\quad + (\zeta_6 G_3(y) + \zeta_4 G_2(y) + \zeta_2 G_1(y))(\tau_{eq} + \tau_{sw}]. \end{aligned} \tag{31}$$

We define $\dot{s}_5$ as follows:

$$\dot{s}_5 = -\epsilon \cdot \mathrm{sat}(s_5), \Rightarrow \dot{V} = s_5 [-\epsilon \cdot \mathrm{sat}(s_5)]. \tag{32}$$

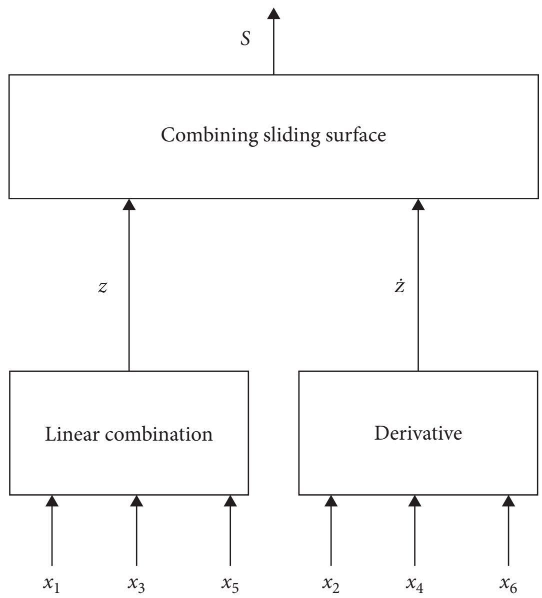

Figure 4: Structure of the aggregated combining surfaces.

From expression of Equations (31) and (32), the switching control is obtained as follows:

$$\tau_{sw} = \frac{-\epsilon \cdot \mathrm{sat}(s_5)}{\zeta_6 G_3(y) + \zeta_4 G_2(y) + \zeta_2 G_1(y)}. \quad (33)$$

3.3. Control Law Based on Combining HSMC. The basic idea behind the combining HSMC method is as follows. The mathematical model of the DRIP system consists of six state variables. These state variables are divided into two groups. One group comprises y_1, y_2, and y_3, while the other groups cover their derivatives. The schematics presentation of combining HSMC is shown in Figure 4.

To design the combining HSMC for DRIP system, we define the intermediate variable z as follows:

$$z = \varrho_1 y_1 + \varrho_2 y_3 + \varrho_3 y_5, \quad (34)$$

$$\dot{z} = \varrho_1 y_2 + \varrho_2 y_4 + \varrho_3 y_6, \quad (35)$$

where ϱ_1, ϱ_2, and ϱ_3 are positive constants. The higher order sliding surface will consist of intermediate variable and its derivative:

$$S = \beta z + \dot{z}. \quad (36)$$

The combining HSMC control law is defined by

$$\tau = \tau_{eq} + \tau_{sw}. \quad (37)$$

The equivalent control law can be obtained by putting $\dot{S} = 0$ as follows:

Table 1: The physical parameters of the model and controllers.

Parameters	Values	Parameters	Values
J_1	0.5741	J_2	96
J_3	0.16	L_1	3
L_2	1	m_2	10
m_3	2	l_2	1
l_3	0.1	g	9.81
c_1	0.65	c_2	1
c_3	21	c_4	1
c_5	51	c_6	1
α_1	1.18	α_2	1.2
α_3	0.35	ϵ	10
ζ_1	0.85	ζ_2	1
ζ_3	3.6	ζ_4	0.4
ζ_5	0.2	ζ_6	1.6
ϱ_1	1	ϱ_2	0.242
ϱ_3	0.64	β	0.487

$$\tau_{eq} = -\frac{\beta\varrho_1 y_2 + \beta\varrho_2 y_4 + \beta\varrho_3 y_6 + \varrho_1 F_1(y) + \varrho_2 F_2(y) + \varrho_3 F_3(y)}{\varrho_1 G_1(y) + \varrho_2 G_2(y) + \varrho_3 G_3(y)}. \quad (38)$$

The switching control law can be obtained from Lyapunov function as follows:

$$V = \frac{1}{2} S^2, \quad (39)$$

and by defining $\dot{S}$ as $\dot{S} = -\epsilon \cdot sat(S)$.

Hence,

$$\tau_{sw} = -\frac{\epsilon \cdot \mathrm{sat}(S)}{\varrho_1 G_1(y) + \varrho_2 G_2(y) + \varrho_3 G_3(y)}. \quad (40)$$

4. Numerical Simulations

The designed HSMC techniques are simulated in the MATLAB Simulink model to verify their feasibility and performance. The physical parameters of the model and controllers are listed in Table 1 (Appendix). The designed controllers successfully stabilize the horizontal and vertical bars. This means that all the designed HSMC techniques are feasible to stabilize the DRIP system. The performance comparison of all designed techniques is shown in Figures 5 and 6.

The response time for all designed control techniques to stabilize the horizontal bar of the DRIP system is shown in Table 2. It can be seen that the aggregated HSMC technique has a much shorter response time than the incremental and combining HSMC technique. It also has less response time as compared to the study of Elkinany et al. [20]. Hence, aggregated HSMC technique is proposed to stabilize the DRIP system.

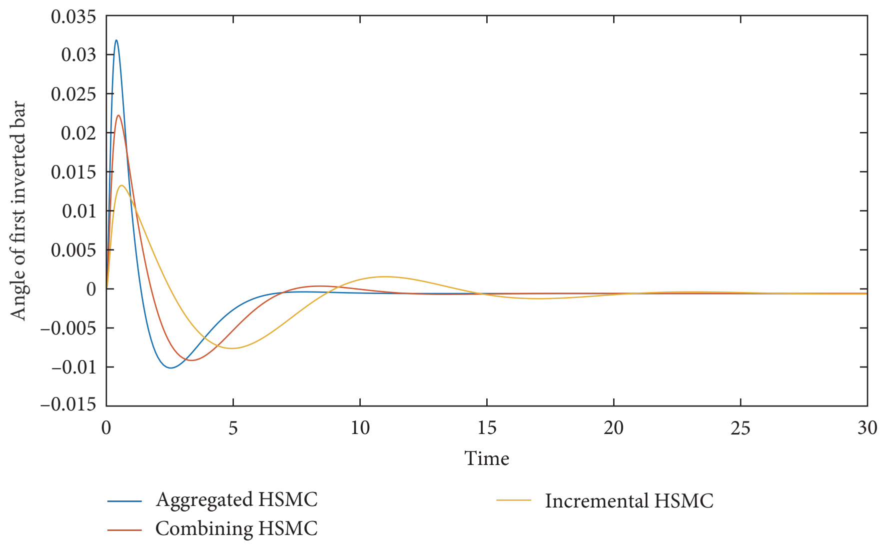

Figure 5: Stabilization of horizontal bar with time starting from initial condition.

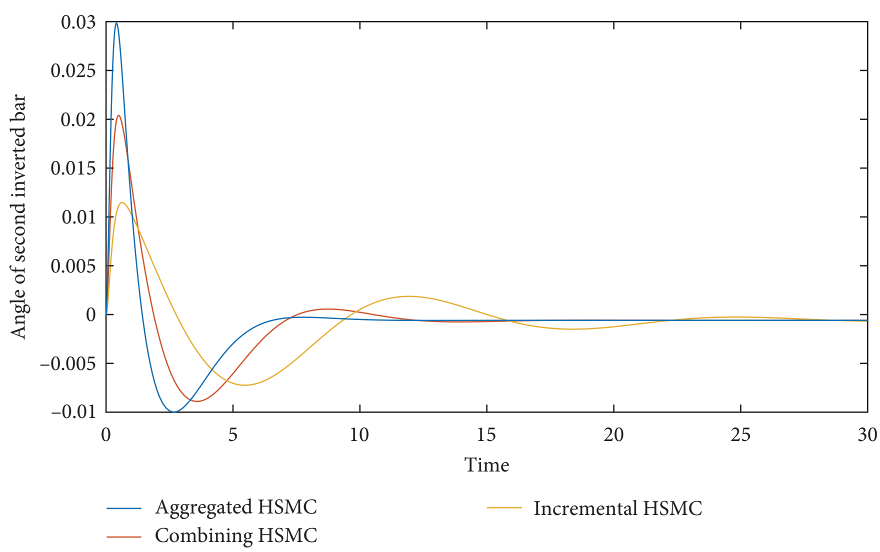

Figure 6: Stabilization of vertical bars with time starting from initial condition.

Table 2: Response time of all three methods to stabilize horizontal bar.

Method	Response time of horizontal bar
Aggregated HSMC	7 s
Combining HSMC	13 s
Incremental HSMC	30 s

5. Conclusion

This article presents a mathematical model of the DRIP system, and HSMC techniques are successfully designed to stabilize the DRIP system. The numerical results demonstrate that all designed controllers can be used to stabilize the DRIP system. However, aggregated HSMC technique has a shorter stabilization time compared to the other two control techniques. Aggregated HSMC for the DRIP system consists of three first-level surfaces and one second-level sliding surface. The first-level sliding surfaces are used to obtain the equivalent controls, while the second-level sliding surface is used to interact with the first-level sliding surfaces and obtain switching control. We use the saturation function and constant switching gain to obtain switching control. In conclusion, aggregated HSMC technique is more efficient in order to stabilize the DRIP system.

Appendix

We have, $H_1 = J_1 + L_1^2(m_2 + m_3)$, $H_2 = L_1(m_2 l_2 + m_3 L_2)$, $H_3 = L_1 m_3 l_3$, $H_4 = J_2 + L_2^2 m_3 + m_2 l_2^2$, $H_5 = L_2 m_3 l_3$, $H_6 = J_3 + l_3^2 m_3$, $H_7 = (m_2 l_2 + m_3 L_2)g$, and $H_8 = m_3 l_3 g$. Then

$$
\begin{aligned}
\Delta &= H_1H_4H_6 - H_2^2H_6\cos^2 y_3 - H_1H_5^2(\cos(y_5 - y_3))^2 - H_3^2H_4\cos^2 y_5\\
&\quad + 2H_2H_3H_5\cos y_3\cos y_5\cos(y_5 - y_3),\\
\alpha_1 &= y_4b_2[H_2H_6\cos y_3 - H_3H_5\cos y_5\cos(y_5 - y_3)]\\
&\quad - y_2b_1[H_4H_6 - H_5^2\cos^2(y_5 - y_3)] + y_6b_3[H_3H_4\cos y_5 - H_2H_5\cos y_3\cos(y_5 - y_3)]\\
&\quad + y_6^2[H_3H_4H_6\sin y_5 - H_3H_5^2\cos^2(y_5 - y_3)\sin y_5 - H_2H_5H_6\cos y_3\sin(y_5 - y_3)\\
&\quad + H_3H_5^2\cos y_5\sin(y_5 - y_3)\cos(y_5 - y_3) + y_4^2[H_2H_4H_6\sin y_3\\
&\quad - H_2H_5^2\sin y_3\cos^2(y_5 - y_3) - H_2H_5^2\cos y_3\sin(y_5 - y_3)\cos(y_5 - y_3)\\
&\quad + H_3H_4H_5\cos y_5\sin(y_5 - y_3)] + H_3H_5H_7\sin y_3\cos y_5\cos(y_5 - y_3)\\
&\quad - H_2H_6H_7\sin y_3\cos y_3 + H_2H_5H_8\cos y_3\sin y_5\cos(y_5 - y_3) - H_3H_4H_8\cos y_5\sin y_5,\\
\alpha_2 &= y_2b_1[H_2H_6\cos y_3 - H_3H_5\cos y_5\cos(y_5 - \cos y_3)] - y_4b_2[H_1H_6 - H_3^2\cos^2 y_5]\\
&\quad + y_6b_3[H_1H_5\cos(y_5 - y_3) - H_2H_3\cos y_3\cos y_5] + y_6^2[H_3^2H_5\cos y_5\sin y_5\cos(y_5 - y_3)\\
&\quad - H_2H_3H_6\cos y_3\sin y_5 - H_3^2H_5\cos^2 y_5\sin(y_5 - y_3) + H_1H_5H_6\sin(y_5 - y_3)]\\
&\quad + y_4^2[H_1H_5^2\sin(y_5 - y_3)\cos(y_5 - y_3) - H_2^2H_6\sin y_3\cos y_3\\
&\quad - H_2H_3H_5\cos y_3\cos y_5\sin(y_5 - y_3) + H_2H_3H_5\sin y_3\cos y_5\cos(y_5 - y_3)]\\
&\quad + H_1H_6H_7\sin y_3 - H_3^2H_7\cos^2 y_5\sin y_3 - H_1H_5H_8\sin y_5\cos(y_5 - y_3)\\
&\quad + H_2H_3H_8\cos y_5\cos y_3\sin y_5,\\
\alpha_3 &= y_4b_2[H_1H_5\cos(y_5 - y_3) - H_2H_3\cos y_3\cos y_5] - y_6b_3(H_1H_6 - H_3^2\cos^2 y_5)\\
&\quad + y_2b_1[H_3H_4\cos y_5 - H_2H_5\cos y_3\cos(y_5 - y_3)] + y_4^2[H_2^2H_5\cos^2 y_3\sin(y_5 - y_3)\\
&\quad - H_1H_4H_5\sin y_5 - H_2\sin y_3(H_3H_4\cos y_5 - H_2H_5\cos y_3\cos(\cos y_5 - y_3))]\\
&\quad + y_6^2[H_2H_3H_5\cos y_3\cos y_5\sin(y_5 - y_3) - H_1H_5^2\sin(y_5 - y_3)\cos(y_5 - y_3)\\
&\quad - H_3^2H_4\sin y_5\cos y_5 + H_2H_3H_5\cos y_3\sin y_5\cos(y_5 - y_3)]\\
&\quad + H_2H_3H_7\sin y_3\cos y_3\cos y_5 - H_1H_5H_7\sin y_3\cos(y_5 - y_3)\\
&\quad + H_1H_4H_8\sin y_5 - H_2^2H_8\sin y_5\cos^2 y_3,
\end{aligned}
\tag{A.1}
$$

$$
\begin{aligned}
\beta_1 &= H_4H_6 - H_5^2\cos^2(y_5 - y_3),\\
\beta_2 &= H_3H_5\cos y_5\cos(y_5 - y_3) - H_2H_6\cos y_3,\\
\beta_3 &= H_2H_5\cos y_3\cos(y_5 - y_3) - H_3H_4\cos y_5.
\end{aligned}
\tag{A.2}
$$

Data Availability

The data used to support the findings of this study are included within the article.

Conflicts of Interest

The authors declare that they have no conflicts of interest.

References

[1] V. I. Utkin and S. K. Korovin, "Application of sliding mode to static optimization," *Automatic Remote Control*, vol. 4, pp. 570–579, 1972.

[2] V. I. Utkin and K. D. Yang, "Methods for construction of discontinuity planes in multidimensional variable structure systems," *Avtomatika i Telemekhanika*, no. 10, pp. 72–77, 1978.

[3] J. Chen, H. Huang, A. G. Cohn, D. Zhang, and M. Zhou, "Machine learning-based classification of rock discontinuity trace: SMOTE oversampling integrated with GBT ensemble learning," *International Journal of Mining Science and Technology*, vol. 32, no. 2, pp. 309–322, 2022.

[4] Z. Huang, D. Zhang, K. Pitilakis et al., "Resilience assessment of tunnels: framework and application for tunnels in alluvial deposits exposed to seismic hazard," *Soil Dynamics and Earthquake Engineering*, vol. 162, Article ID 107456, 2022.

[5] M. Idrees, S. Ullah, and S. Muhammad, "Sliding mode control design for stabilization of underactuated mechanical systems," *Advances in Mechanical Engineering*, vol. 11, no. 5, 2019.

[6] K. Furuta, M. Yamakita, and S. Kobayashi, "Swing-up control of inverted pendulum using pseudo-state feedback," *Proceedings of the Institution of Mechanical Engineers, Part I: Journal of Systems and Control Engineering*, vol. 206, no. 4, pp. 263–269, 1992.

[7] J. J. Choi and J. S. Kim, "Robust control for rotational inverted pendulums using output feedback sliding mode controller and disturbance observer," *KSME International Journal*, vol. 17, pp. 1466–1474, 2003.

[8] P. Pakdeepattarakorn, P. Thamvechvitee, J. Songsiri, M. Wongsaisuwan, and D. Banjerdpongchai, "Dynamic models of a rotary double inverted pendulum system," in *2004 IEEE Region 10 Conference TENCON 2004*, vol. 4, pp. 558–561, IEEE, Chiang Mai, Thailand, 2004.

[9] J. Driver and D. Thorpe, *Design, Build and Control of a Single/Double Rotational Inverted Pendulum*, The University of Adelaide, School of Mechanical Engineering, Australia, 2004.

[10] V. Casanova, J. Salt, R. Piza, and A. Cuenca, "Controlling the double rotary inverted pendulum with multiple feedback delays," *International Journal of Computers Communications & Control*, vol. 7, no. 1, pp. 20–38, 2012.

[11] B. Li, "*Rotational Double Inverted Pendulum*," PhD thesis, University of Dayton, 2013.

[12] A. Jose, C. Augustine, S. M. Malola, and K. Chacko, "Performance study of PID controller and LQR technique for inverted pendulum," *World Journal of Engineering and Technology*, vol. 3, no. 2, pp. 76–81, 2015.

[13] M. Yue, C. An, Y. Du, and J. Sun, "Indirect adaptive fuzzy control for a nonholonomic/underactuated wheeled inverted pendulum vehicle based on a data-driven trajectory planner," *Fuzzy Sets and Systems*, vol. 290, pp. 158–177, 2016.

[14] J. Wen, Y. Shi, and X. Lu, "Stabilizing a rotary inverted pendulum based on logarithmic lyapunov function," *Journal of Control Science and Engineering*, vol. 2017, Article ID 4091302, 11 pages, 2017.

[15] X. Liu, A. N. Vargas, X. Yu, and L. Xu, "Stabilizing two-dimensional stochastic systems through sliding mode control," *Journal of the Franklin Institute*, vol. 354, no. 14, pp. 5813–5824, 2017.

[16] M. Idrees, S. Muhammad, and S. Ullah, "Robust hierarchical sliding mode control with state-dependent switching gain for stabilization of rotary inverted pendulum," *Kybernetika*, vol. 55, no. 3, pp. 455–471, 2019.

[17] A. H. D. Markazi, M. Maadani, S. H. Zabihifar, and N. Doost-Mohammadi, "Adaptive fuzzy sliding mode control of under-actuated nonlinear systems," *International Journal of Automation and Computing*, vol. 15, pp. 364–376, 2018.

[18] Y. A Butt, "Robust stabilization of a class of nonholonomic systems using logical switching and integral sliding mode control," *Alexandria Engineering Journal*, vol. 57, no. 3, pp. 1591–1596, 2018.

[19] I. M. Mehedi, U. M. Al-Saggaf, R. Mansouri, and M. Bettayeb, "Stabilization of a double inverted rotary pendulum through fractional order integral control scheme," *International Journal of Advanced Robotic Systems*, vol. 16, no. 4, 2019.

[20] B. Elkinany, M. Alfidi, R. Chaibi, and Z. Chalh, "T–S fuzzy system controller for stabilizing the double inverted pendulum," *Advances in Fuzzy Systems*, vol. 2020, Article ID 8835511, 9 pages, 2020.